



Downscaling the MODIS land surface temperature using a trapezoidal concept applied to the MODIS and sentinel 2 images

Zohreh Faraji · Abbas Kaviani · Leila Khosravi

Received: 15 December 2023 / Accepted: 8 June 2024 / Published online: 27 June 2024
© The Author(s), under exclusive licence to Springer Nature Switzerland AG 2024

Abstract Downscaling methods are crucial for accessing high-resolution thermal data simultaneously. The DisTRAD model is commonly used for downscaling thermal images, but changes in soil moisture, such as those caused by irrigation operations, can lead to errors in the process. This study investigated the potential use of TOTRAM and OPTRAM models to reduce errors in LST downscaling in irrigated fields. Sentinel satellite imagery was utilised to enhance the resolution of MODIS Land Surface Temperature (LST) from 1000 to 20 m in the fields of Megsal and Hezarjofla agro-industrial company in Qazvin province. Soil moisture was estimated using the OPTRAM model, and the results were compared with observational data. The findings indicated that on days with NDVI greater than 0.6, the R^2 value exceeded 0.88 and the RMSE value was less than $0.06 \text{ cm}^3/\text{cm}^3$. Then, MODIS LST

images were downscaled to 20 m using codes in Google Earth Engine (GEE). Evaluation was conducted using observational data from collected land surface temperature data for 36 points. Comparison of the downscaled LST data with observational data on days with irrigation revealed a decrease in MAE and RMSE error indices by approximately 0.4 and 1.2 degrees Celsius, respectively, in the OPTRAM-TPTRAM model compared to the DisTRAD model. Consequently, the OPTRAM-TOTRAM model generally outperforms the DisTRAD model in LST downscaling. Lastly, it is recommended to assess the TOTRAM and OPTRAM models for downscaling MODIS sensor LST in other irrigated fields.

Keywords OPTRAM model · TOTRAM model · DisTRAD model · Soil moisture

Z. Faraji
Water Science and Engineering Dept., Faculty
of Agriculture and Natural Resources, Imam Khomeini
International University, Qazvin, Iran
e-mail: zfaraji9101@gmail.com

A. Kaviani (✉)
Associate Professor of Water Science and Engineering
Dept., Faculty of Agriculture and Natural Resources,
Imam Khomeini International University, Qazvin, Iran
e-mail: Abbasskaviani@gmail.com

L. Khosravi
Irrigation and Reclamation Engineering Dept., College
of Agriculture and Natural Resources, University
of Tehran, Karaj, Iran
e-mail: 14011eila.khosravi@gmail.com

Introduction

Land surface temperature (LST) plays a crucial role in the exchange of heat flux and long-wave infrared radiation (LWIR) between the Earth's surface and atmosphere. It is a key parameter for understanding surface energy and water balance processes at local and global scales (Li et al., 2013). Various studies have demonstrated the potential of LST, particularly in applications related to thermal infrared data. Satellites like AVHRR, MODIS, and Landsat provide data with different resolutions and temporal coverage to estimate surface temperature. Thermal infrared data complements other remote sensing

information and is unique in identifying ground materials and features, including thermal anomalies, rock types, and soil moisture (Prakash et al., 1997). While MODIS enhances continuous Earth monitoring with daily temporal resolution, its spatial resolution (1 km) may not be adequate for analysing areas with high spatial heterogeneity in terms of topography and land cover. In contrast, thermal images from high spatial resolution scanners on satellites like Landsat 5 and Landsat 8 offer better detection of spatial patterns (Allan et al., 2016; Semmens et al., 2016; Xing et al., 2015). Despite this, the current satellite tools still have limitations. This is due to the fact that while many satellites offer data with high spatial resolution, they have low temporal resolution (Allan et al., 2016; Anderson et al., 2007; Carpintero et al., 2016; Park et al., 2004; Xing et al., 2015).

Based on the information presented, there is a high demand for thermal images with both high spatial and temporal resolution in agricultural and land management fields (Weng et al., 2014). The Downscaling technique is commonly used to enhance the spatial resolution of Land Surface Temperature (LST) data, drawing on biophysical properties obtained from remote sensing data at a higher spatial resolution (Bala et al., 2020; Essa et al., 2012; Wang et al., 2020). This method leverages the correlation between images with high spatial resolution but low temporal resolution and those with low spatial resolution but high temporal resolution to produce images with both high spatial and temporal resolutions. To accurately depict thermal changes on the earth's surface, data with high spatial resolution such as visible and infrared bands, spectral indices, digital elevation models, and land use information are essential (Maeda, 2014; Bindhu et al., 2013; Bisquert et al., 2016; Essa et al., 2017; Lillo-Saavedra et al., 2018).

The "trapezoid" or "triangle" model is a common approach in remote sensing for estimating soil moisture through optical and thermal data. The Thermal-Optical TRapezoid model (TOTRAM) interprets pixel distribution in the LST-VI space, where LST represents land surface temperature and VI is a vegetation cover index based on remote sensing. Despite its apparent success, TOTRAM has limitations. To address these, Sadeghi et al., (2015) introduced a TRapezoidal model called OPTRAM, based on a physical relationship between soil moisture and shortwave infrared transformed reflectance (STR). OPTRAM does not require thermal bands and can be directly used for estimating soil moisture from satellite observations without thermal

bands, such as Sentinel-2. Furthermore, OPTRAM only requires one parameterization for the study area, overcoming the limitations of the TOTRAM model (Sadeghi et al., 2017). Various methods have been developed to downscale LST from the MODIS sensor, but they often lack accuracy in irrigated areas due to large moisture variations (Gao et al., 2012). Therefore, this study investigates the potential of using a combination of TOTRAM and OPTRAM models to downscale MODIS LST from 1000 to 20 m using Sentinel satellite, aiming to improve the accuracy of downscaling. Since 2003, numerous studies have been conducted in the field of downscaling MODIS LST images.

Kustas et al. (2003) found that DisTrad can estimate subpixel thermal values at the MODIS NDVI pixel resolution with around 1.5 °C uncertainty. The DisTARD method involves a simple linear regression between NDVI and LST, which is its main advantage. However, a limitation of the DisTRAD method is the neglect of other variables such as soil moisture changes. To address this, the TsHARP model was introduced, based on the DisTRAD method but using a regression relationship between T_s and F_c instead of NDVI (Agam et al., 2007). While the TsHARP method outperforms DisTRAD to some extent, it has not fully overcome its disadvantages. In 2012, a new data mining system (DMS) was introduced to extend the application of downscaling thermal image methods in more complex conditions. This method uses a tree regression between TIR brightness temperature and shortwave spectral reflectance. Evaluation of the DMS and TsHARP methods using Landsat satellite images in dryland and irrigated fields showed that changes in soil moisture due to irrigation increase errors in downscaling thermal images. Statistical analysis indicated the superiority of the DMS method over the TsHARP method (Gao et al., 2012). However, the issue of errors caused by soil moisture changes in the process of downscaling LST still persists. Recent research studies in this field highlight the need to incorporate soil moisture or a soil moisture-sensitive index as an input to downscaling models for the MODIS sensor (Sánchez et al., 2020). Therefore, the use of soil moisture estimation models in irrigated regions may help reduce errors caused by these changes by considering them in calculations.

The Temperature-Vegetation Dryness Index (TVDI) is a widely used method for estimating soil moisture without relying on observational data. It

is based on the relationship between Land Surface Temperature (LST) and Normalized Difference Vegetation Index (NDVI). The introduction of this index marked a significant advancement in understanding soil moisture conditions at the ground surface. Spatial variations in the TVDI index show a 70% correlation coefficient between model data and TVDI, allowing for soil moisture changes to be observed at a finer scale than with hydrological models (Sandholt et al., 2002).

To address the limitations of the TOTRAM model, Sadeghi et al. (2017) proposed the OPTRAM model. This model is based on the linear physical relationship between soil moisture and shortwave infrared transformed reflectance (STR), and is parameterized according to pixel distribution within the STR-VI space. Ambrosone et al. (2020) further evaluated soil moisture using the OPTRAM model with Sentinel-2 satellite images. The Pearson test results indicate a significant statistical correlation between observed and estimated soil moisture values (Ambrosone et al., 2020). Additionally, the OPTRAM model provides soil moisture estimates close to observational data, while also highlighting low estimates of soil moisture from surface soil moisture (SSM 1km) during the growing season.

The LST parameter plays a crucial role in the water and energy balance equations (Kalma et al., 2008), impacting the spatial resolution of evapotranspiration images and the effective management of water resources in farms (Ibrahim et al., 2022). Studies on sensitivity analysis highlight the significant influence of the LST parameter on ET estimation models such as SEBAL and SEBS (Gibson et al., 2011; Weng, 2009; Rocha et al., 2020; Abid et al., 2019). Even a small change in the LST value can lead to notable variations in ET estimation, emphasising the importance of accurate input variables, particularly LST, for precise ET estimation. Furthermore, an increase in global temperature can have adverse effects on crop yields, making it essential to explore soil moisture estimation models like TOTRAM and OPTRAM based on remote sensing to mitigate errors arising from significant moisture changes during LST downscaling in irrigated fields. This research aims to evaluate the accuracy of soil moisture estimation data from the OPTRAM model by comparing it with observational data. It also

seeks to explore the potential of using soil moisture estimation models TOTRAM and OPTRAM to minimize errors resulting from moisture fluctuations during the fine-scale LST scaling process in irrigated regions. Additionally, it aims to assess the effectiveness of the proposed method on days when irrigation activities have taken place.

Materials and methods

Study area

This research encompasses the Maghsal and Hazarjelfa Agro-industrial companies in Qazvin city, Qazvin province, Iran. The Maghsal agro-industrial site is situated at 35° 9' N and 60° 10' 12'' E, with an average elevation of 1220 m above sea level. The area experiences a cold and dry Mediterranean climate, with an average annual rainfall of 298 mm. Covering around one thousand hectares, the soil in this area is categorised as loamy clay. The primary products cultivated include wheat, canola, barley, forage corn, and dry alfalfa, with irrigation carried out using sprinkler systems like linear and centre-pivot irrigation. The Hazarjelfa agro-industrial company spans approximately 850 hectares, positioned at 35° 1' N and 60° 11' E. Similar to Maghsal, this company shares comparable soil texture and agricultural product diversity. Figure 1 illustrates an aerial perspective of the study area and its location in Qazvin city.

Data was collected randomly over a 15-day period from July 3rd to September 28th, 2022, in the study area during the summer cultivation period for corn. The observational data gathered includes land surface temperature, air temperature, soil moisture at a depth of 5 cm, irrigation, and weather conditions. The Testo 868 thermal sensor was used to collect land surface temperature data, while the HH2 soil moisture meter from DELTA-T Company was used to measure soil moisture. Additionally, 5 Sentinel satellite images corresponding to the data collection dates were obtained. The distribution maps of ground-based LST measurements is illustrated in the Fig. 2 and The details of data collection dates, the number of data collection points on each date (N), and the average air temperature in the study area are presented in Table 1.

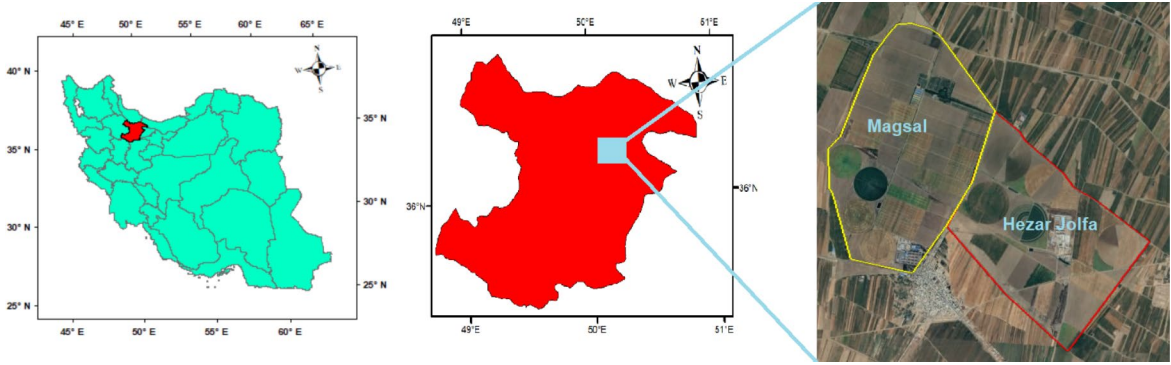


Fig. 1 Aerial image of the study area and its location in Qazvin province

Fig. 2 The distribution maps of ground-based LST measurements

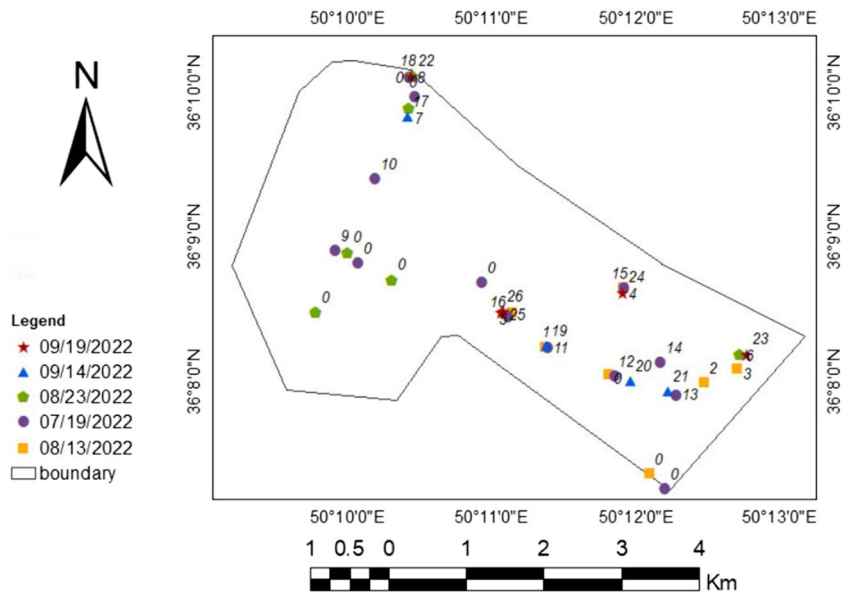


Table 1 List of data collection dates, the number of data collection points on each date (N)

Date	N	Ta (C°)
19-Jul-2022	13	37.2
13-Aug-2022	7	39.6
23-Aug-2022	6	29.3
14-Sep-2022	5	25.7
19-Sep-2022	5	29.5

MODIS sensor and sentinel satellite

The Terra satellite was launched from the Vandenberg Air Force Base in the United States on December 18, 1999, and commenced gathering data from the Earth on February 24, 2000. It is equipped with several sensors capable of capturing various types of images depicting different characteristics of the Earth’s surface. One of these sensors is the MODIS

sensor, which can produce images with spatial resolutions of 250 m, 500 m, and 1 km (Kelly et al., 2014). The daily LST data from the MODIS sensor has been available as a free archive from 2000 to the present. However, a significant challenge lies in the low spatial resolution (1000 m) of its thermal images. Consequently, the process of downscaling these images from 1000 to 20 m represents a crucial advancement in enhancing their usability. The Sentinel series satellites are developed and engineered by the European Union, with 6 series of these satellites launched into space thus far. The Sentinel-2 satellite is specifically designed for forest monitoring, assessing changes in land cover, managing natural disasters, and calculating physical indices and variables, and it is equipped with 13 spectral bands (Phiri et al., 2020).

This research utilised images from level 2 of the Sentinel-2A satellite, which lacks a thermal band but offers suitable spatial resolution (10 and 20 m) and a temporal resolution of 5 days with its visible and near-infrared images. The study investigates the potential of using these images in the TOTRAM and OPTRAM soil moisture estimation models to downscale MODIS thermal sensor images to a 20 m level. The study employed MOD11A1 and MOD09GA data from the MODIS sensor, as well as bands 4, 8, and 12 from the Sentinel satellite. The image specifications are detailed in Table 2. It is important to note that data collection occurred on various days at different times between 8 am and 5 pm, while the MODIS sensor passed over the study area around 1 pm.

DisTrade

In 2003, Kustas et al. developed the DisTrad technique to scale down land surface radiometric

temperature images. This technique relies on an empirical correlation between the normalized difference vegetation index (NDVI) as the predictor and land surface radiometric temperature (TR) as the outcome. The correlation is represented by Eq. 1.

$$\check{T}_{R1000}(NDVI_{1000}) = a + bNDVI_{1000} + cNDVI_{1000}^2 \tag{1}$$

The calculated radiometric temperature (°C) is denoted as \check{T}_{R1000} , and $NDVI_{1000}$ represents the aggregated normalized difference vegetation index. In this study, a linear regression relationship ($c=0$) is utilised to minimise errors. By substituting $NDVI_{250}$ with $NDVI_{1000}$ in Eq. 1, TR_{250} (downscaled radiometric temperature) is derived. However, it is important to note that this approach does not factor in temperature variations resulting from changes in soil moisture, as the least squares regression method only accounts for average conditions. To tackle this issue, the standard deviation of observed regressions at a 1000 m scale is adjusted (Eq. 2).

$$\Delta\check{T}_{R1000} = T_{R1000} - \check{T}_{R1000} \tag{2}$$

The TR_{1000} refers to the calculated radiometric temperature. Subsequently, the radiometric temperature of each pixel (i) is determined using Eq. 1 and Eq. 3.

$$\check{T}_{R250}(i) = \check{T}_{R1000}(NDVI_{250}(i)) + \Delta\check{T}_{R1000} \tag{3}$$

TOTRAM model

The TOTRAM model utilises the pixel distribution in the LST-VI space. By eliminating pixels with clouds and water bodies, the scatter plot of pixels forms a triangular or trapezoidal shape (Carlson, 2013).

Table 2 Specifications of MODIS and sentinel satellite images

Wavelength range (nm)	Temporal resolution (day)	Spatial resolution(m)	Product/Bands	Satellite
650–680	5	10	Band 4 (Red)	Sentinel
785–899	5	10	Band 8 (NIR)	
2100–2280	5	20	Band 12 (SWIR)	
—	daily	500	MOD09GA	Terra/MODIS
—	daily	1000	MOD11A1	

The normalized difference vegetation index (NDVI) is the most frequently used vegetation cover index in TOTRAM, calculated using Eq. 4.

$$NDVI = \frac{R_{nir} - R_{red}}{R_{nir} + R_{red}} \tag{4}$$

Which R_{nir} is the reflectance of the near-infrared band and R_{red} is the reflectance of the red band. The inverse linear relationship between soil moisture (θ) and land surface temperature (LST) is shown in Eq. 5.

$$W = \frac{\theta - \theta_d}{\theta_w - \theta_d} = \frac{LST_d - LST}{LST_d - LST_w} \tag{5}$$

Which W is the normalized soil moisture value, θ_d is the minimum value of soil moisture in dry local conditions, θ_w is the maximum value of soil moisture in moist local conditions, and LST_d and LST_w are the land surface temperature ($^{\circ}C$) at the dry and moist edges, respectively LST_d and LST_w are shown in Fig. 3. The upper (dry) and lower (moist) edges of the trapezoid are used to estimate LST_d and LST_w for each NDVI. LST_d and LST_w are calculated by Eqs. 6 and 7.

$$LST_d = id + sdNDVI \tag{6}$$

$$LST_w = iw + swNDVI \tag{7}$$

Equations 5, 6 and 7 are combined to estimate the soil moisture value for each pixel as a function of NDVI and LST.

$$TOTRAM = \frac{id + sdNDVI - LST}{id - iw + (sd - sw)NDVI} \tag{8}$$

OPTRAM model

The Kubelka and Munk model, initially introduced in 1931, was later expanded by Sadeghi et al. in 2015. This physical model demonstrates the linear correlation between soil moisture and shortwave infrared transformed reflectance (STR). It relies on the distribution of pixels in the NDVI-STR. In contrast to the TOTRAM model, it utilises optical data rather than thermal data, as detailed in Eqs. 9, 10, 11, 12 and 13.

$$W = \frac{\theta - \theta_d}{\theta_w - \theta_d} = \frac{STR - STR_d}{STR_w - STR_d} \tag{9}$$

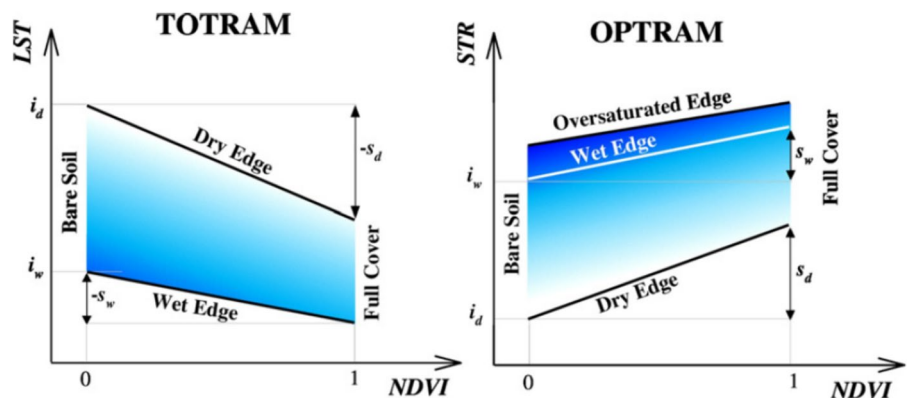
The term "STR" denotes shortwave infrared transformed reflectance, while "STRw" and "STRd" represent the shortwave infrared transformed reflectance at the wet and dry edges, respectively. The calculation for STR is based on Eq. 10, where R_{SWIR} represents the reflectance of the SWIR band.

$$STR = \frac{(1 - R_{SWIR})^2}{2R_{SWIR}} \tag{10}$$

The parameters of Eq. 9 can be extracted from satellite images for the desired range of wet and dry edges, and the edges can be defined based on the visual inspection of pixel distribution (Carlson, 2013).

$$STR_d = id + sdNDVI \tag{11}$$

Fig. 3 Parameters of TOTRAM and OPTRAM models (Sadeghi et al., 2017)



$$STR_w = iw + swNDVI \tag{12}$$

Which *id* represents the minimum STR; *sd* represents the minimum vegetation cover density; *iw* represents the maximum STR; *sw* represents the maximum vegetation cover density. The OPTRAM model is obtained by Eq. 13, which can estimate soil moisture in the visible wavelength range.

$$OPTRAM = \frac{id + sdNDVI - STR}{id - iw + (sd - sw)NDVI} \tag{13}$$

Downscaling method

To downscale the Land Surface Temperature (LST) data from the MODIS sensor, the TOTRAM and OPTRAM models are initially implemented in Google Earth Engine. Subsequently, the coefficients of the TOTRAM and OPTRAM equations are individually obtained for each date. Following this, NDVI

and STR indices are derived using Sentinel satellite images, and soil moisture images are generated using the OPTRAM model with a spatial resolution of 20 m. The Sentinel satellite images of soil moisture and NDVI are then integrated into the TOTRAM equation, resulting in the production of LST with a spatial resolution of 20 m.

For downscaling the LST from the MODIS sensor using the DisTRAD model, the 1000 m LST image from the MODIS sensor and the 20 m NDVI image from the Sentinel satellite for the study area are clipped. Subsequently, the NDVI image is aggregated from 20 to 1000 m. The coefficients of the linear regression equation are derived using the 1000 m LST and NDVI images. Next, the values of $\Delta\check{T}1000$ and $\check{T}R20$ (NDVI_20) are calculated, and finally, the downscaled LST value from the DisTRAD model is determined by summing these values. The research method's flowchart, outlining each step, is presented in Fig. 4.

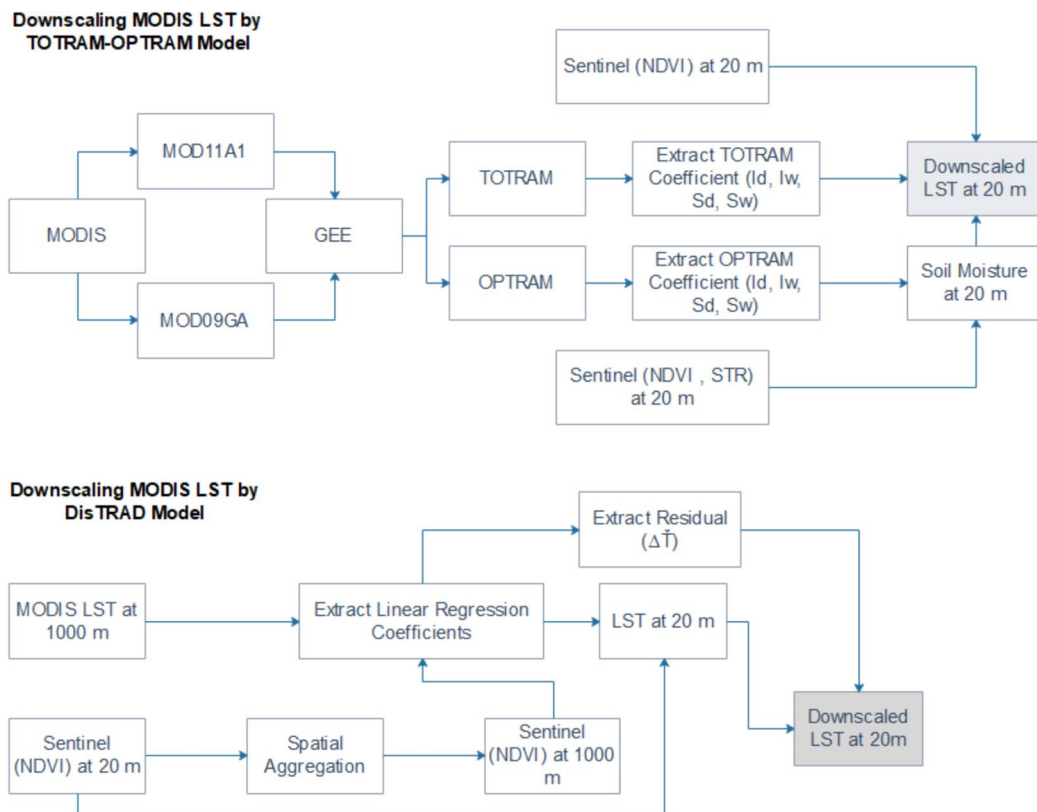


Fig. 4 Flowchart of the steps for performing the LST scaling process

Data calibration

To calibrate the downscaled data with the observational data, 70% of the total 36 data points were utilised to derive the equation, while the remaining 30% were allocated for validation.

Error measurement indices

One of the statistical indices used to evaluate model performance is correlation coefficient, which is defined by Eq. 14:

$$r = \frac{\sum_{i=1}^n (P_i - P)(O_i - O)}{\sqrt{\sum_{i=1}^n (P_i - P)^2 (O_i - O)^2}} \quad (14)$$

The correlation coefficient (r) represents the relationship between predicted (P_i) and observed (O_i) values over a period of n years. It ranges between 1 and -1, indicating the degree of match between the trends of observed and predicted values. Additional quantitative indices for evaluation are root mean square error (RMSE), mean bias error (MBE), and mean absolute error (MAE).

$$RMSE = \sqrt{\frac{\sum (C_i - M_i)^2}{n}} \quad (15)$$

$$MBE = \frac{\sum (C_i - M_i)}{n} \quad (16)$$

$$MAE = \frac{\sum |C_i - M_i|}{n} \quad (17)$$

When C_i represents the calculated value, M_i represents the observed value, and n represents the number of data points. An RMSE, MAE, and MBE of zero or close to zero indicate high accuracy

in the method used. As the distance from zero increases, the method's accuracy decreases.

Results and discussion

Soil moisture

The omission of soil moisture changes in the scaling equations has been identified as a significant source of error in LST scaling results by Kustas et al., 2003, Agam et al., 2007, Gao et al., 2012, and Sánchez et al., 2020. In this study, the OPTRAM model is utilised to estimate soil moisture and facilitate the scaling of LST measurements from the MODIS sensor. The evaluation of the OPTRAM model's ability to estimate soil moisture utilised observational data, with the results presented in Table 3. The findings indicate that on specific dates with an average NDVI value at the sampling points exceeding 0.6, the R^2 value is greater than 0.88, and the RMSE value is less than $0.06 \text{ cm}^3/\text{cm}^3$ (e.g. August 13, September 14, and September 19). Conversely, on July 19 and August 23, with lower average NDVI values at the sampling points (0.29 and 0.27, respectively), the R^2 value is lower, and the RMSE value is higher. Previous studies have established a direct relationship between NDVI and soil moisture, with higher soil moisture corresponding to increased NDVI values. It is anticipated that lower reported NDVI values will align with lower soil moisture values. However, on July 19 and August 23, when the volumetric soil moisture for the sampling points exceeds 36% and 32% respectively, the NDVI values for the points are approximately 0.29 and 0.27. This discrepancy may be attributed to variations in sampling timing and non-uniform NDVI conditions at the sampled points. Nevertheless, the overall results support the

Table 3 Statistical evaluation of the results obtained from the OPTRAM model and observational data of soil moisture

Date	R2	RMSE(cm^3/cm^3)	MAE(cm^3/cm^3)	MBE(cm^3/cm^3)	NDVI
19-Jul	0.4	0.16	0.12	-0.06	0.29
13-Aug	0.92	0.07	0.05	0.05	0.71
23-Aug	0.38	0.22	0.22	-0.15	0.27
14-Sep	0.88	0.09	0.06	0.05	0.68
19-Sep	0.99	0.05	0.05	0.03	0.67

conclusion that the OPTRAM model effectively estimates soil moisture.

The TOTRAM model utilises the correlation between NDVI and LST to predict soil moisture. By having the soil moisture and NDVI values for each pixel, the model estimates the LST value. In this research, the OPTRAM model was employed to predict soil moisture and facilitate the adjustment of LST measurements from the MODIS sensor. By substituting the soil moisture derived from the OPTRAM model into the TOTRAM model equation, LST was estimated for each pixel with a spatial resolution of 20 m. The reason for using soil moisture from the OPTRAM model lies in its independence from the LST parameter. While the TOTRAM model directly utilises LST to predict soil moisture, it overlooks variations in soil moisture due to irrigation in irrigated areas. Conversely, the OPTRAM model uses the STR parameter instead of LST. Furthermore, according to Ambrosone et al. (2020), TOTRAM performs better

in arid regions, whereas OPTRAM performs better in irrigated regions. Therefore, incorporating the estimated soil moisture from the OPTRAM model can account for changes in soil moisture resulting from irrigation in the LST adjustment process.

Figure 5 depicts the LST image obtained by the MODIS sensor (1000 m) and the downscaled LST image generated by the DisTRAD and OPTRAM-TOTRAM models on September 19, 2022. It is evident that the LST image from the MODIS sensor (1000 m) only covers 18 pixels of the entire region, whereas the downscaled LST images (b and c) exhibit a marked visual enhancement compared to the MODIS sensor's LST image (a). Notably, the downscaled image from the DisTRAD model clearly displays the 1000-m pixel border. While the thermal images from the MODIS sensor offer valuable long-term information essential for climate change studies, they do not provide suitable data at the farm scale or for investigating spatial changes. Therefore,

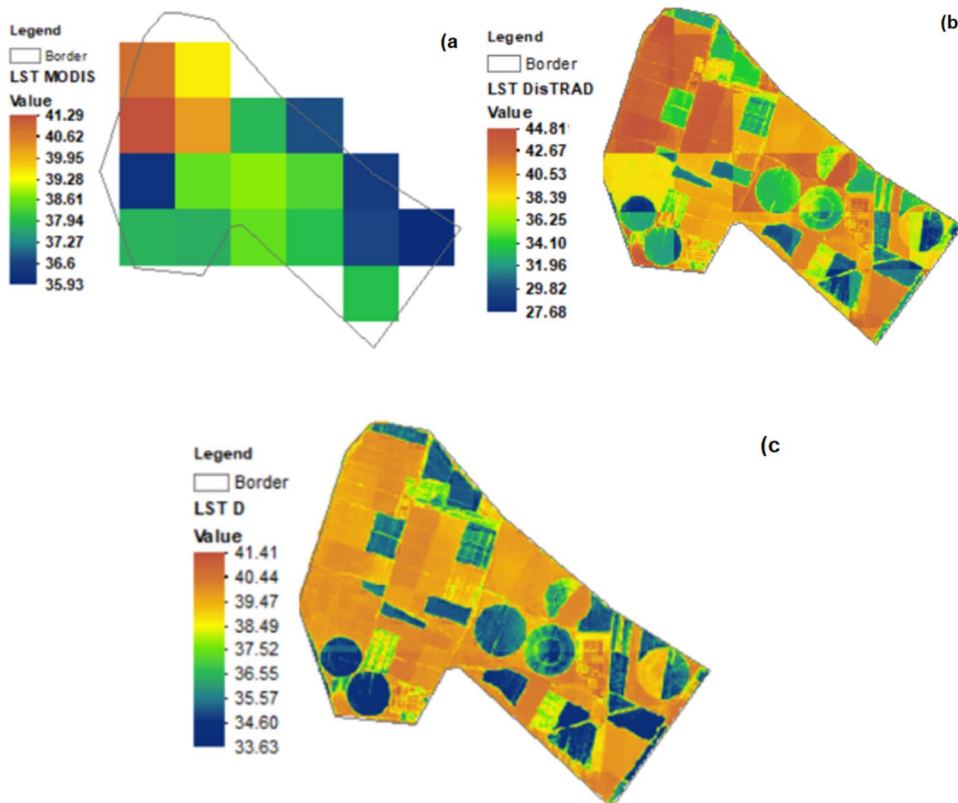


Fig. 5 Shows **a**) the LST image obtained from the MODIS sensor (1000 m) and **b**) the downscaled LST image obtained from the DisTRAD and **c**) OPTRAM-TOTRAM models on September 19, 2022

Table 4 Statistical analysis results of the downscaled LST compared to the MODIS sensor data (1000 m)

Date	RMSE-(C°)	OPTRAM-TOTRAM			RMSE (C°)	DisTRAD		
		MBE (C°)	MAE (C°)	R ²		MBE (C°)	MAE (C°)	R ²
7/19/2022	0.67	0.19	0.52	0.49	3.7	0.75	2.74	0.49
8/13/2022	1.26	0.98	1.11	0.69	2.73	-0.5	2.38	0.55
8/23/2022	1.69	0.83	1.43	0.51	4.41	-2.65	3.79	0.13
9/14/2022	1.54	1.06	1.53	0.64	2.36	0.48	1.37	0.72
9/19/2022	1.95	0.43	1.64	0.91	3.4	0.6	2.75	0.85

downscaling these images at the farm scale holds significant importance in agricultural management.

To assess the downscaled LST images in comparison to the MODIS LST images, statistical indices such as R², RMSE, MAE, and MBE were utilised (see Table 4). The findings reveal that the RMSE values for the OPTRAM-TOTRAM model range from 0.67 to 1.97 degrees Celsius, with MBE values ranging from 0.19 to 1.06 degrees Celsius. For the DisTRAD model, the RMSE values range from 2.36 to 4.4 degrees Celsius, and the MBE values range from -2.65 to 0.75 degrees Celsius. These results demonstrate a strong correlation between the downscaled images from the OPTRAM-TOTRAM model and the original

MODIS sensor images, with an RMSE value of less than 2 degrees Celsius. Conversely, higher RMSE values are observed in the DisTRAD model, indicating superior performance of the OPTRAM-TOTRAM model. Notably, on August 23, the DisTRAD model exhibited lower performance compared to other days. The data collected before and after irrigation, as shown in Table 3, resulted in non-uniform conditions, leading to higher errors in both soil moisture estimation and LST downscaling on this date. However, the use of the OPTRAM-TOTRAM model in downscaling LST has significantly mitigated this issue, demonstrating much better performance than the DisTRAD model on August 23.

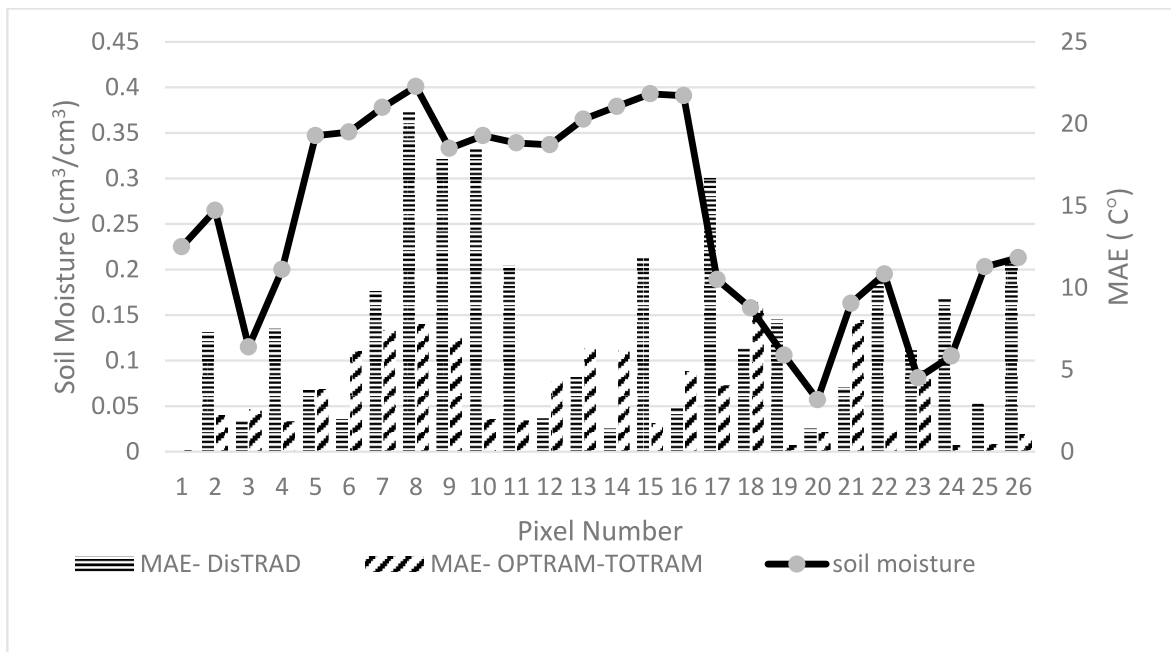


Fig. 6 Changes in MAE value compared to soil moisture changes for the DisTRAD and OPTRAM-TOTRAM models

Statistical analysis by observational data

Due to the low number of sampling points on some days, all collected data points were utilized for statistical analysis. However, in certain areas, conditions had changed since the satellite passing time, leading to the removal of some points, resulting in 26 remaining points, as shown in Fig. 6 by "Pixel Number". Pixels number 1 to 26 in Fig. 2 are shown. Points labeled with 0 are those points that have been deleted due to the mismatch between the observed data time and the satellite passing time. To examine the impact of soil moisture changes on the mean absolute error (MAE) measurement in the DisTRAD and OPTRAM-TOTRAM models, the MAE value was compared to the observed soil moisture. Figure 6 illustrates that, generally, the MAE value in the OPTRAM-TOTRAM model is lower than in the DisTRAD model. It is also evident that in some areas, as soil moisture increases, the MAE value in the DisTRAD model increases significantly. The MAE value in the OPTRAM-TOTRAM model appears to have less correlation with soil moisture changes. The LST parameter is influenced by various factors such as wind speed, duration of solar radiation, solar radiation angle, humidity, air temperature, and vegetation cover, in addition to soil moisture changes, which also impact the changes in the MAE value. Nevertheless, the notable point is the lesser impact of soil moisture changes on the MAE value in the OPTRAM-TOTRAM model compared to the DisTRAD model.

Table 5 Statistical analysis results of the downscaled LST data for the OPTRAM-TOTRAM and DisTRAD models

Model	RMSE (C°)	MBE (C°)	R ²
OPTRAM-TOTRAM	3.4	0.17	0.9
DisTRAD	9.09	-0.8	0.55

Figure 6 and 7 display the scatter plot of downscaled LST data and observational data for the OPTRAM-TOTRAM and DisTRAD models, respectively. LST D represents downscaled land surface temperature, while LST O represents observational data for land surface temperature. A clear linear relationship between these data is evident. The statistical analysis results for both models are presented in Table 5. For the OPTRAM-TOTRAM model, the R², RMSE, and MBE values are calculated as 0.9, 3.4 degrees Celsius, and 0.17 degrees Celsius, respectively, indicating significantly better performance than the DisTRAD model. Additionally, irrigated points (LST I) are identified in Figs. 7 and 8, as soil moisture significantly affects errors in the LST image scaling process. The results demonstrate a decrease in the MAE and RMSE error measurement indices by approximately 0.4 and 1.2 degrees Celsius, respectively, for the OPTRAM-TOTRAM model compared to the DisTRAD model on days when irrigation was carried out. Therefore, the results indicate superior performance of the OPTRAM-TOTRAM model, even on days with irrigation.

Fig. 7 Shows the scatter plot of the downscaled LST data and the observed data (OPTRAM-TOTRAM model)

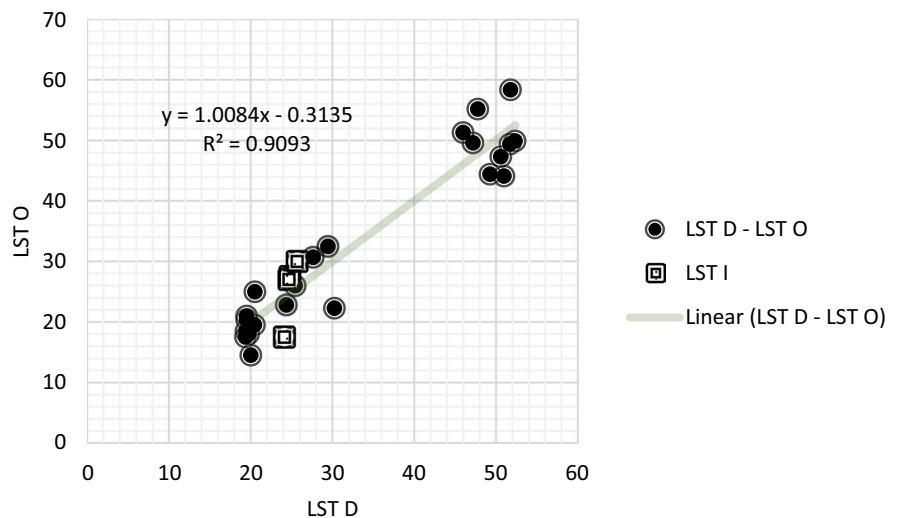
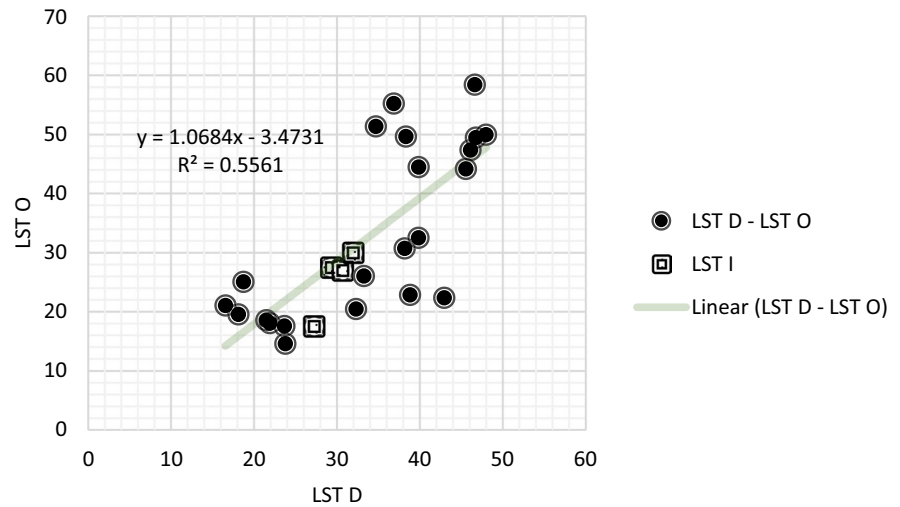


Fig. 8 Shows the scatter plot of the downscaled LST data and the observed data (DisTRAD model)



Conclusions

This research aimed to explore the potential use of the TOTRAM and OPTRAM soil moisture estimation models for refining the LST data from the MODIS sensor in irrigated areas. The findings suggest that combining these models can effectively enhance the resolution of MODIS sensor data to 20 m using Sentinel satellite images. The OPTRAM-TOTRAM model emerges as a superior method for refining LST sensor data compared to the DisTRAD model in the study area. Variations in soil moisture and non-uniform data acquisition times pre and post irrigation were identified as key factors contributing to errors in LST refinement. However, the results demonstrate that the OPTRAM-TOTRAM model significantly mitigates these issues and outperforms the DisTRAD model under similar conditions. Furthermore, the study reveals that on irrigation days, the MAE and RMSE error indices decreased by approximately 0.4 and 1.2 degrees Celsius, respectively, for the OPTRAM-TOTRAM model compared to the DisTRAD model. Thus, indicating the superior performance of the OPTRAM-TOTRAM model even on irrigation days.

Author contributions Kaviani A. and Faraji Z. wrote the main manuscript text and Khosravi L. and Kaviani A. provide the field Data. All authors reviewed the manuscript.

Funding No funding was received to assist with the preparation of this manuscript. All costs were covered by the authors.

Data availability Data generated during the study are included in the manuscript.

Competing interests The authors declare no competing interests.

Declarations All authors have read, understood, and have complied as applicable with the statement on "Ethical responsibilities of Authors" as found in the Instructions for Authors.

Ethics approval Not relevant.

Consent to participate Not relevant.

Consent for publication Not relevant.

Conflict of interest The authors declare no conflict of interest.

References

- Abid, N., Mannaerts, C., & Bargaoui, Z. (2019). Sensitivity of actual evapotranspiration estimation using the sebs model to variation of input parameters (LST, DSSF, aerodynamics parameters, LAI, FVC). *The International Archives of Photogrammetry, Remote Sensing and Spatial Information Sciences*, 42, 1193–1200. <https://doi.org/10.5194/isprs-archives-XLII-2-W13-1193-2019>
- Agam, N., Kustas, W. P., Anderson, M. C., Li, F., & Neale, C. M. (2007). A vegetation index based technique for spatial sharpening of thermal imagery. *Remote Sensing of Environment*, 107(4), 545–558. <https://doi.org/10.1016/j.rse.2006.10.006>
- Allan, M. G., Hamilton, D. P., Trolle, D., Muraoka, K., & McBride, C. (2016). Spatial heterogeneity in geothermally-influenced lakes derived from atmospherically corrected Landsat thermal

- imagery and three-dimensional hydrodynamic modelling. *International Journal of Applied Earth Observation and Geoinformation*, 50, 106–116. <https://doi.org/10.1016/j.jag.2016.03.006>
- Ambrosone, M., Matese, A., Di Gennaro, S. F., Gioli, B., Tudoroiu, M., Genesio, L., Miglietta, F., Baronti, S., Maienza, A., & Ungaro, F. (2020). Retrieving soil moisture in rainfed and irrigated fields using Sentinel-2 observations and a modified OPTRAM approach. *International Journal of Applied Earth Observation and Geoinformation*, 89, 102113. <https://doi.org/10.1016/j.jag.2020.102113>
- Anderson, M. C., Norman, J. M., Mecikalski, J. R., Otkin, J. A., & Kustas, W. P. (2007). A climatological study of evapotranspiration and moisture stress across the continental United States based on thermal remote sensing: 1. Model formulation. *Journal of Geophysical Research: Atmospheres*, 112(D10117). <https://doi.org/10.1029/2006JD007506>
- Bala, R., Prasad, R., & Yadav, V. P. (2020). Thermal sharpening of MODIS land surface temperature using statistical downscaling technique in urban areas. *Theoretical and Applied Climatology*, 141(3), 935–946. <https://doi.org/10.1007/s00704-020-03253-w>
- Bindhu, V., Narasimhan, B., & Sudheer, K. (2013). Development and verification of a non-linear disaggregation method (NL-DisTrad) to downscale MODIS land surface temperature to the spatial scale of Landsat thermal data to estimate evapotranspiration. *Remote Sensing of Environment*, 135, 118–129. <https://doi.org/10.1016/j.rse.2013.03.023>
- Bisquert, M., Sánchez, J. M., & Caselles, V. (2016). Evaluation of disaggregation methods for downscaling MODIS land surface temperature to Landsat spatial resolution in Barax test site. *IEEE Journal of Selected Topics in Applied Earth Observations and Remote Sensing*, 9(4), 1430–1438. <https://doi.org/10.1109/JSTARS.2016.2519099>
- Carlson, T. N. (2013). Triangle models and misconceptions. *International Journal of Remote Sensing*, 3(3), 155–158.
- Carpintero, E., Dugo, M. G., Hain, C., Nieto, H., Gao, F., Andreu, A., Kustas, W., Anderson, M. (2016, October). Continuous evapotranspiration monitoring and water stress at watershed scale in a Mediterranean oak savanna. In *Remote Sensing for Agriculture, Ecosystems, and Hydrology XVIII* (vol. 9998, pp. 190–206). <https://doi.org/10.1117/12.2241521>
- Essa, W., Verbeiren, B., van der Kwast, J., Van de Voorde, T., & Batelaan, O. (2012). Evaluation of the DisTrad thermal sharpening methodology for urban areas. *International Journal of Applied Earth Observation and Geoinformation*, 19, 163–172. <https://doi.org/10.1016/j.jag.2012.05.010>
- Essa, W., Verbeiren, B., Van der Kwast, J., & Batelaan, O. (2017). Improved DisTrad for downscaling thermal MODIS imagery over urban areas. *Remote Sensing*, 9(12), 1243. <https://doi.org/10.3390/rs9121243>
- Gao, F., Kustas, W. P., & Anderson, M. C. (2012). A data mining approach for sharpening thermal satellite imagery over land. *Remote Sensing*, 4(11), 3287–3319. <https://doi.org/10.3390/rs4113287>
- Gibson, L., Münch, Z., & Engelbrecht, J. (2011). Particular uncertainties encountered in using a pre-packaged SEBS model to derive evapotranspiration in a heterogeneous study area in South Africa. *Hydrology and earth system sciences*, 15(1), 295–310. https://ui.adsabs.harvard.edu/link_gateway/2011HESS...15..295G/doi:10.5194/hess-15-295-2011
- Ibrahim, T. I., Al-Maliki, S., Salameh, O., Waltner, I., & Vekerd, Z. (2022). Improving LST Downscaling Quality on Regional and Field-Scale by Parameterizing the DisTrad Method. *ISPRS International Journal of Geo-Information*, 11(6), 327. <https://doi.org/10.3390/ijgi11060327>
- Kalma, J. D., McVicar, T. R., & McCabe, M. F. (2008). Estimating land surface evaporation: A review of methods using remotely sensed surface temperature data. *Surveys in Geophysics*, 29(4), 421–469. <https://doi.org/10.1007/s10712-008-9037-z>
- Kelly, A., Moyer, E., Mantziaras, D., & Case, W. (2014). Terra mission operations: Launch to the present (and beyond). *Earth Observing Systems XIX*, 9218, 180–191. <https://doi.org/10.1117/12.2061253>
- Kubelka, P., & Munk, F. (1931). A contribution to the optics of pigments. *Z Technology and Physics*, 12(593), 193.
- Kustas, W. P., Norman, J. M., Anderson, M. C., & French, A. N. (2003). Estimating subpixel surface temperatures and energy fluxes from the vegetation index–radiometric temperature relationship. *Remote Sensing of Environment*, 85(4), 429–440. [https://doi.org/10.1016/S0034-4257\(03\)00036-1](https://doi.org/10.1016/S0034-4257(03)00036-1)
- Li, Z.-L., Tang, B.-H., Wu, H., Ren, H., Yan, G., Wan, Z., Trigi, I., & Sobrino, J. A. (2013). Satellite-derived land surface temperature: Current status and perspectives. *Remote Sensing of Environment*, 131, 14–37. <https://doi.org/10.1016/j.rse.2012.12.008>
- Lillo-Saavedra, M., García-Pedrero, A., Merino, G., & González-Martín, C. (2018). Ts2urf: A new method for sharpening thermal infrared satellite imagery. *Remote Sensing*, 10(2), 249. <https://doi.org/10.3390/rs10020249>
- Maeda, E. E. (2014). Downscaling MODIS LST in the East African mountains using elevation gradient and land-cover information. *International Journal of Remote Sensing*, 35(9), 3094–3108. <https://doi.org/10.1080/01431161.2014.903442>
- Park, S., Feddema, J. J., & Egbert, S. L. (2004). Impacts of hydrologic soil properties on drought detection with MODIS thermal data. *Remote Sensing of Environment*, 89(1), 53–62. <https://doi.org/10.1016/j.rse.2003.10.003>
- Phiri, D., Simwanda, M., Salekin, S., Nyirenda, V. R., Murayama, Y., & Ranagalage, M. (2020). Sentinel-2 data for land cover/use mapping: A review. *Remote Sensing*, 12(14), 2291. <https://doi.org/10.3390/rs12142291>
- Prakash, A., Gupta, R., & Saraf, A. K. (1997). A Landsat TM based comparative study of surface and subsurface fires in the Jharia coalfield, India. *International Journal of Remote Sensing*, 18(11), 2463–2469. <https://doi.org/10.1080/014311697217738>
- Rocha, N. S. D., Käfer, P. S., Skokovic, D., Veeck, G., Diaz, L. R., Kaiser, E. A., & Roberti, D. R. (2020). The Influence of Land Surface Temperature in Evapotranspiration Estimated by the S-SEBI Model. *Atmosphere*, 11(10), 1059. <https://doi.org/10.3390/atmos11101059>
- Sadeghi, M., Jones, S. B., & Philpot, W. D. (2015). A linear physically-based model for remote sensing of soil moisture using short wave infrared bands. *Remote Sensing of*

- Environment*, 164, 66–76. <https://doi.org/10.1016/j.rse.2015.04.007>
- Sadeghi, M., Babaeian, E., Tuller, M., & Jones, S. B. (2017). The optical trapezoid model: A novel approach to remote sensing of soil moisture applied to Sentinel-2 and Landsat-8 observations. *Remote Sensing of Environment*, 198, 52–68. <https://doi.org/10.1016/j.rse.2017.05.041>
- Sánchez, J. M., Galve, J. M., González-Piqueras, J., López-Urrea, R., Niclòs, R., & Calera, A. (2020). Monitoring 10-m LST from the Combination MODIS/Sentinel-2, validation in a high contrast semi-arid agroecosystem. *Remote Sensing*, 12(9), 1453. <https://doi.org/10.3390/rs12091453>
- Sandholt, I., Rasmussen, K., & Andersen, J. (2002). A simple interpretation of the surface temperature/vegetation index space for assessment of surface moisture status. *Remote Sensing of Environment*, 79(2–3), 213–224. [https://doi.org/10.1016/S0034-4257\(01\)00274-7](https://doi.org/10.1016/S0034-4257(01)00274-7)
- Semmens, K. A., Anderson, M. C., Kustas, W. P., Gao, F., Alfieri, J. G., McKee, L., & Yang, Y. (2016). Monitoring daily evapotranspiration over two California vineyards using Landsat 8 in a multi-sensor data fusion approach. *Remote Sensing of Environment*, 185, 155–170. <https://doi.org/10.1016/j.rse.2015.10.025>
- Wang, S., Luo, X., & Peng, Y. (2020). Spatial downscaling of MODIS land surface temperature based on geographically weighted autoregressive model. *IEEE Journal of Selected Topics in Applied Earth Observations and Remote Sensing*, 13, 2532–2546. <https://doi.org/10.1109/JSTARS.2020.2968809>
- Weng, Q. (2009). Thermal infrared remote sensing for urban climate and environmental studies: Methods, applications, and trends. *ISPRS Journal of photogrammetry and remote sensing*, 64(4), 335–344. <https://doi.org/10.1016/j.isprsjprs.2009.03.007>, <https://www.sciencedirect.com/science/article/abs/pii/S092427160900046X>
- Weng, Q., Fu, P., & Gao, F. (2014). Generating daily land surface temperature at Landsat resolution by fusing Landsat and MODIS data. *Remote Sensing of Environment*, 145, 55–67. <https://doi.org/10.1016/j.rse.2014.02.003>
- Xing, Q., Li, L., Lou, M., Bing, L., Zhao, R., & Li, Z. (2015). Observation of oil spills through landsat thermal infrared imagery: A case of deepwater horizon. *Aquatic Procedia*, 3, 151–156. <https://doi.org/10.1016/j.aqpro.2015.02.205>

Publisher's Note Springer Nature remains neutral with regard to jurisdictional claims in published maps and institutional affiliations.

Springer Nature or its licensor (e.g. a society or other partner) holds exclusive rights to this article under a publishing agreement with the author(s) or other rightsholder(s); author self-archiving of the accepted manuscript version of this article is solely governed by the terms of such publishing agreement and applicable law.